ACS OMEGA

http://pubs.acs.org/journal/acsodf

Article

Interface Effects on Magnetic Flux Pinning in $La_{0.7}Sr_{0.3}MnO_3/YBa_2Cu_3O_{7-x}$ Bilayers

Sayan Chaudhuri, You-Sheng Chen, and Jauyn Grace Lin*

Cite This: *ACS Omega* 2023, 8, 16694−16699

Read Online

ACCESS | Metrics & More | Article Recommendations

ABSTRACT: The magnetic pinning properties of a ferromagnet/superconductor hybrid structure consisting of a $La_{0.7}Sr_{0.3}MnO_3$(LSMO) layer with various thicknesses on top of a fixed thickness $YBa_2Cu_3O_{7-x}$ (YBCO) layer are investigated in this article. The existence of a weakly magnetic layer was identified at the interface between YBCO and LSMO by a ferromagnetic resonance (FMR) study. Magnetic moment and anisotropy of the interfacial layer were probed using the angular-dependent FMR study. This layer gives rise to an additional flux pinning contribution to the bulk magnetic pinning from the LSMO layer. Our study provides insight into the complex interface physics in the LSMO/YBCO bilayer system, promoting a new pathway for the development of novel flux pinning-related functionality.

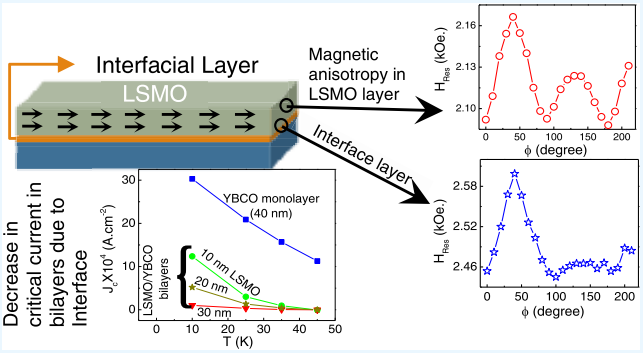

INTRODUCTION

The proximity effect in a superconductor (SC)/ferromagnet (FM) hybrid system has garnered great interest due to novel physics phenomena and the potential to exploit them in the promising avenue of superconducting spintronics.[1,2] The interaction between superconductivity and ferromagnetism in these systems leads to a competition between different order states and a reconstruction of structural coupling between the two layers, which projects a large impact on the superconducting performance by affecting the magnetization dynamics.[3−5] Combination of a d-wave high-temperature superconductor $YBa_2Cu_3O_7$ (YBCO) and half-metallic manganites like $La_{0.67}Ca_{0.33}MnO_3$ (LCMO) or $La_{0.67}Sr_{0.33}MnO_3$ (LSMO) has been the most studied SC/FM oxide system.[6−8] There are diversified results regarding the appearance of spin-triplet supercurrent and the interplay of superconductivity and ferromagnetism in these bilayer systems. Some studies were successful to improve the flux pinning and superconducting properties via generating spin-triplet supercurrent,[9−11] and several recent experiments revealed that the electronic interaction, proximity effect, or a "magnetic dead layer" at the interface can affect the related properties.[12−17] The properties and effects of the interfacial layer have been studied extensively, and some interesting results have been reported, such as the appearance of perpendicular magnetic anisotropy in an in-plane anisotropic LSMO film,[8] the suppression of superconductivity,[18] the appearance of spin-triplet supercurrent,[11] etc. The origin of this dead layer is not properly understood and has much scope for debate. In addition to intrinsic effects like interfacial strain, electron transfer from LSMO to YBCO, and possible orbital reconstruction,[15,16] some extrinsic factors like chemical intermixing, oxygen or cation vacancies, and structural defects can be named as some of the reasons for the formation of this layer.[17] Considerable research has also been carried out to describe the characteristic of the interfacial layer and to modulate its effect on the overall superconductivity of the system.[7,19−21]

Ferromagnetic resonance (FMR) measurement is one of the most efficient techniques to study the interface properties since it is capable of resolving magnetic signals coming from the interface layer and the rest of the bulk FM layer. This technique has been successfully employed to study the heterogeneous nature of magnetization at the interface of LSMO thin film originating from substrate-induced strain.[22] In this work, we report and analyze the flux pinning properties of LSMO/YBCO bilayers and investigate the interfacial magnetic properties by using both static magnetometric measurements and dynamic FMR technique. We also probe the symmetry of magnetic domains by using angular-dependent FMR spectra, which provide important insight into the possible interfacial pinning mechanism.

Received: December 13, 2022
Accepted: March 20, 2023
Published: May 1, 2023

EXPERIMENTAL PROCEDURE

A 40 nm thick single-layer YBCO film, a series of LSMO(t) films with t = 10−40 nm, and LSMO/YBCO bilayers with YBCO bottom layer were deposited on LSAT(001) substrates using a pulsed laser deposition system. The targets of LSMO and YBCO were ablated by using a KrF (248 nm) excimer laser at a repetition rate of 1 Hz. The LSAT substrate temperature during the deposition was 750 °C in all cases, whereas the oxygen pressure was 75 mTorr during the growth of YBCO and 300 mTorr for LSMO layer growth. All of the films were annealed with 700 Torr oxygen at 750 °C for 1 h postdeposition. Depending on the thickness of the LSMO layer, the bilayer samples are denoted as LYt40 (t = 10, 20, 30, 40). For comparison, monolayers of LSMO and YBCO were also prepared using the same procedure.

The phase purity and lattice parameter were determined by X-ray diffraction (XRD) measurement using θ−2θ scans with Cu Kα source radiation (λ = 1.541 Å). Temperature- and field-dependent magnetization measurements were carried out using a magnetic property measurement system (MPMS, Quantum design). The critical current density of the samples was evaluated from the magnetic isotherms using an extended Bean's critical state model.[23]

For the FMR measurements, a microwave source provided by the Bruker EMX system with a fixed frequency of 9.8 GHz was used. During the measurement, the system temperature was fixed at room temperature, and the external magnetic field, H, was applied parallel to the sample surface and along the various out- and in-plane orientations of the applied field. The value of θ is defined as the angle between the normal to the film surface with the applied field direction. On the other hand, ϕ indicates the in-plane rotation of the applied field.

RESULTS AND DISCUSSION

The XRD profiles of the bilayer and monolayer films are depicted in Figure 1a, clearly showing that all prepared films are single-phase and c-axis oriented. Lattice parameters of the samples were calculated using Bragg's law ($2d \sin\theta = n\lambda$). The bulk c-axis lattice parameter of YBCO is 1.168 nm[4] (a = 0.382 nm and b = 0.388), whereas pseudocubic LSMO has a bulk lattice parameter $a_\perp$ = 0.387 nm. In our current samples, the 40 nm LSMO film deposited on the LSAT substrate has the $a_\perp$ parameter of 0.396 nm, slightly higher than the bulk value. The smaller lattice parameter of LSAT substrate (0.386 nm, lattice mismatch ∼0.26%) induces compressive strain in the ab plane of the film, and as a result, strain is relaxed along the c-axis. On the other hand, no such change in lattice parameter is observed in the case of the bilayer system, even though YBCO has a much higher lattice parameter and lattice mismatch (∼1.7%), which can be regarded as a discrepancy in the degree of local structural distortions.

Figure 1b shows the temperature dependence of magnetization curves for all of the bilayer samples measured in zero-field cooling (ZFC) and field-cooled (FC) mode (in the inset(c)) with 100 Oe magnetic field, applied perpendicular to the film surface. The negative magnetization observed in the low-temperature region of the ZFC curves exhibits the Meissner effect, indicating a dominant superconducting state below T_{SC}. Above T_{SC}, a positive magnetic moment is observed in ZFC due to the ferromagnetic ordering of the LSMO layer. On the other hand, a positive magnetic moment is observed throughout the measured temperature range in the case of FC

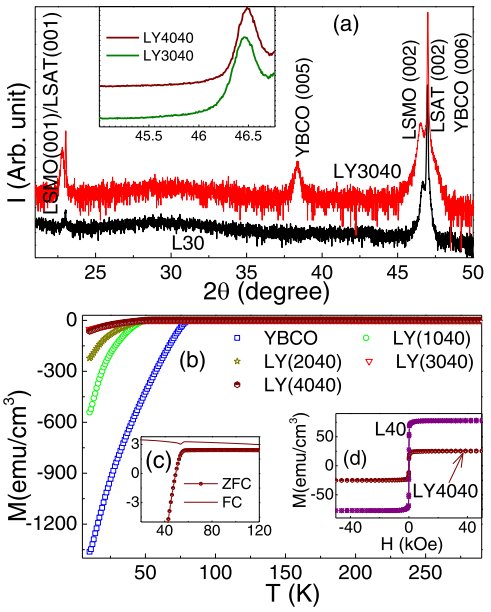

Figure 1. (a) XRD profiles of monolayer LMSO and bilayer LSMO/YBCO samples. The inset shows the LSMO(002) peak. (b) Temperature dependence of M(T) curves in zero-field cooling (ZFC). Inset (c): ZFC and FC curves in the LY3040 film and inset (d): MH curves in a bilayer and monolayer sample.

measurement. A clear degradation of T_{SC} with the increase in LSMO thickness is evident in Figure 1b. In the monolayer YBCO film, the T_{SC} is ∼84 K, which is reduced to ∼52 K in the case of the LY1040 sample. The T_{SC} values decreased again and maintained at 48 K for further increase in the LSMO layer thickness.

In an SC/FM system, superconducting current can tunnel into the FM layer and the corresponding Cooper pairs experience an exchange interaction, which suppresses the superconducting order parameters in the FM layer with the length scale, $\xi_F = \frac{\hbar v_F}{\Delta E_x}$, where v_F is the Fermi velocity and ΔE_x is the exchange splitting. Due to the large value of ΔE_x in LSMO (5.5 eV),[24] the length scale of ξ_F becomes very small (∼1 nm). Therefore, a change in T_{SC} due to the proximity effect in our samples is highly unlikely. On the other hand, the presence of a heterogeneous magnetic layer at the interface can affect the superconducting layer upto a certain length scale. Changing the thickness of the LSMO layer does not affect the thickness of this interfacial layer, and thus, the T_{SC} remains unchanged. Hence, the behavior of T_{SC} in the current case indicates the presence of magnetic inhomogeneity at the interface between YBCO and LSMO. The magnetic inhomogeneity also decreases the overall magnetization as can be seen from the magnetization versus applied field curves for an LSMO monolayer (40 nm) and its bilayer counterpart (LY4040) measured at 100 K temperature presented in the inset (d) of Figure 1. A clear degradation of the magnetization can be observed in the bilayer systems.

Next, we investigated the effect of LSMO capping on the critical current density (j_c) of 40 nm YBCO film. The plots of the field dependence of j_c at 10 K temperature are shown in Figure 2a, which decreases consistently with the increase in LSMO thickness over the whole temperature range of the superconducting phase (see the j_c vs T plots in the inset of Figure 2a). The change in j_c with the LSMO thickness implies

https://doi.org/10.1021/acsomega.2c07928
ACS Omega 2023, 8, 16694−16699

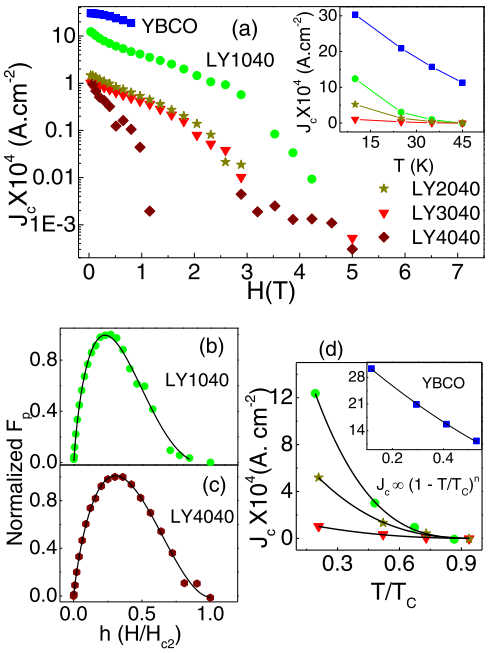

Figure 2. (a) Field dependence of critical current density for the bilayer samples along with 40 nm YBCO monolayer sample at 10 K. The inset shows the temperature variation of zero-field j_c. (b, c) Normalized flux pinning force F_p/F_{pmax} plotted against the reduced field $h = H/H_{C2}$ at 10 K for two bilayer films. The solid lines are corresponding fitting results to the theoretical Dew−Hughes scaling of flux pinning. (d) Temperature dependences of zero-field critical current density for bilayer and pure YBCO films (in the inset). Solid lines are fit to the data.

a clear change in the pinning mechanism. The flux pinning mechanisms of the bilayer samples are analyzed using the quantitative fittings of the flux pinning forces F_p ($F_p = j_c \times H$) to the Dew−Hughes description,[25] $F_p/F_{pmax} = h^p(1 - h)^q$, where p and q are the scaling exponents and h is the applied magnetic field divided by the upper critical field (H_{C2}) of the system. H_{C2} for each system was estimated by extrapolating the j_c vs H curve till $j_c = 0$. Figure 2b,c presents the scaling of normalized pinning force as a function of h (H/H_{C2}) for two bilayer samples at 10 K and the solid line indicates the Dew−Hughes fitting to the experimental data. For the LY1040 sample, the fittings are scaled with $p \sim 0.8$ and $q \sim 2.71$. As the thickness of the LSMO layer increases, completely different behavior is observed, where corresponding scaling parameters are $p \sim 0.9$ and $q \sim 2.1$ for LY2040, $p \sim 0.86$ and $q \sim 2.1$ for LY3040, and $p \sim 0.86$ and q ~ 2.0 for LY4040. The results show a minor change in p-value with a huge variation in the q parameter. Surely, the q parameter plays an important role in suppressing the overall superconductivity with a magnetic field. Oh et al.[26] have shown that flux pinning in the FM/SC heterostructure is governed by the interaction of vortices with pinning sites induced by structural defects in addition to magnetic pinning. The structural disorder of the CuO_2 planes at the interface due to coupling between the FM and SC layer acts as additional pinning mechanism. This hybrid pinning mechanism promotes a large change in the q parameter while not affecting the value of p. In our bilayer systems, the magnetic defect at the interface plays an important role in decreasing the superconducting properties. Similar behavior has been seen in the case of LSMO/GdBCO bilayer samples.[26,27] The variation of p and q parameters indicates that the defect contribution is maximum when the LSMO thickness is 10 nm. As the LSMO layer becomes thicker, magnetization in the ferromagnetic layer increases, which enhances the magnetic pinning in these bilayer samples.

To further understand the inherent mechanism influencing the critical current density in these bilayer systems, the temperature dependence of j_c has been investigated. According to the theory of Blatter et al.,[28] applicable in the framework of single vortex pinning, the temperature dependence of j_c in type II superconductors with small grain boundaries or polycrystalline films can be expressed as $j_c = j_0[1 - T/T_C]^n$ with n as the power factor, dependent on the pinning mechanism.[29] Figure 2c shows the temperature dependence of the zero-field critical current density of the YBCO monolayer and LSMO/YBCO bilayer films with the fits to the above function. The obtained value of $n = 1.6$ for the YBCO monolayer is very close to the theoretically expected value of 3/2.[29] The n value quickly increases to 3.13 for the LY1040 sample and then becomes stable at ∼2.5 for the rest of the bilayer samples. The value of n indicates the robustness of the pinning centers against temperature, where higher n signifies weak pinning. Thus, a higher n value in the LY1040 bilayer signifies the presence of weak pinning centers, which become slightly stronger with the increase in LSMO thickness. An increase in the thickness of the LSMO layer increases the magnetization of the FM layer, which in turn strengthens the magnetic pinning. A similar conclusion has been found from the analysis of field dependence of critical current.

Next, we performed room-temperature FMR measurements on the single-layer LSMO and bilayer systems to gain information on the magnetic properties of the interfacial layer. Figure 3a shows the FMR signals of the bilayer samples while applying the field parallel to the film surface. The bilayer

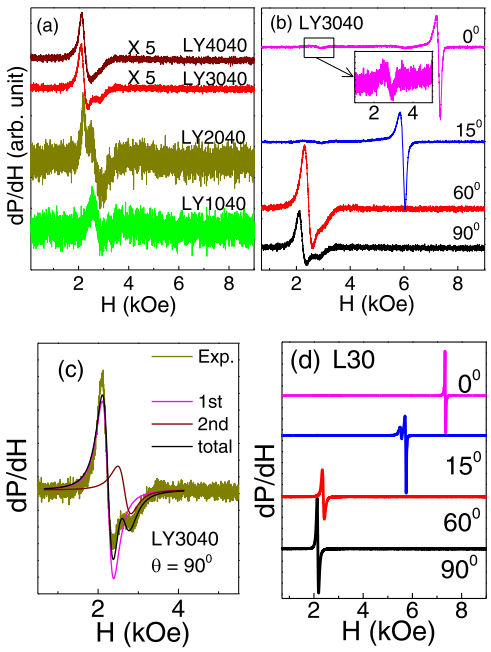

Figure 3. Room-temperature FMR signal of the LSMO/YBCO bilayer (a) for $\theta = 90°$ and (b) different orientations of θ. (c) Fitting of the FMR signal of a nominal bilayer sample is shown. (d) Evolution of the FMR signal in an LSMO monolayer film for different out-of-plane orientations of H.

https://doi.org/10.1021/acsomega.2c07928
ACS Omega 2023, 8, 16694−16699

films exhibit multiple resonance lines, partially overlapping each other.

Since YBCO is nonmagnetic and LSMO monolayers mostly show a single FMR signal, the secondary resonance lines possibly arise from the heterogeneous magnetic layer at the interface. The presence of this layer was also evident from our magnetization measurement. FMR signals obtained while varying the out-of-plane field direction for a monolayer LSMO film are shown in Figure 3b. LSMO monolayers show a single resonance line in the parallel orientation of the magnetic field but show a secondary FMR line slightly separated from the major signal when the magnetic field is oriented in an out-of-plane direction as evident from Figure 3d. The appearance of a second resonance line in the single-layer LSMO film has been observed earlier and originates from small magnetic heterogeneity near the substrate due to substrate-induced strain.[22]

FMR resonance field (H_{res}) of the measured signals was extracted by fitting the data with the first derivative of the Lorentzian equation. A superposition of two functions was used when more than one FMR signal is observed. The dependence of calculated H_{res} parameters for both of the modes on θ_H for a nominal single-layer LSMO film and bilayer sample is shown in Figure 4a,b. In bilayer samples, the first

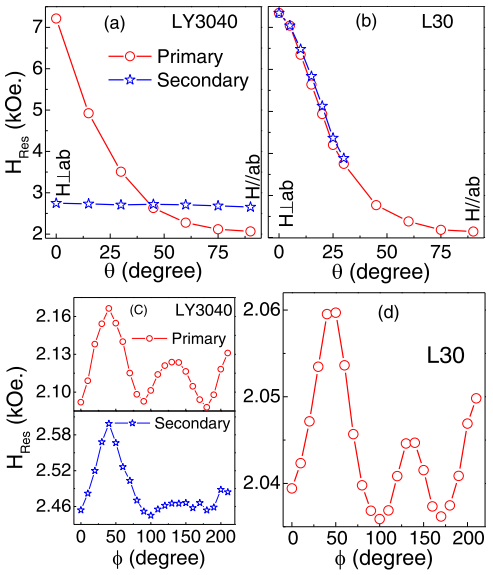

Figure 4. (a) Variation of H_{res} in the LY3040 bilayer and (b) 30 nm LSMO monolayer sample for the out-of-plane orientation of the magnetic field. (c) Variation of H_{res} in the LY3040 bilayer and (d) 30 nm LSMO monolayer sample for the in-plane orientation of the magnetic field.

mode shifts to higher H_{Res} as the applied field changes from in-plane to out-of-plane, whereas the second mode remains at an almost similar position (shown in the inset of Figure 3b). On the other hand, in the case of the single-layer LSMO sample, a second mode only appears when $\theta_H \geq 10°$, closely follows the behavior of the primary signal, and overlaps on it when $\theta_H \geq 30°$. Generally, Kittel formulas with appropriate demagnetizing field (M_0) and magnetoelastic coupling field are used to describe the resonance condition in FM films

$$\left(\frac{\omega}{\gamma}\right)^2 = [H_\perp - 4\pi M_0 + 2B_1(e_z - e_x)/M_0] \times [H_\perp - 4M_0 + 2B_1(e_x - e_y)/M_0] \quad (1)$$

$$\left(\frac{\omega}{\gamma}\right)^2 = [H_{\backslash\backslash} - +2B_1(e_z - e_x)\ /\ M_0] \times [H_\backslash + 4M_0 - 2B_1(e_x + e_y)\ /\ M_0] \quad (2)$$

where $H_\perp$ and $H_{\backslash\backslash}$ represent the H_{res} for the applied field perpendicular and parallel to the film plane, respectively, $4\pi M_0$ is the demagnetizing field, B_1 is the longitudinal magnetoelastic coupling constant, and e_is are the components along x, y, and z directions. For a strain-relaxed FM film, where B_1 is very small, eqs 1 and 2 can be simplified as

$$\omega/\gamma = [H_\perp - 4\pi M_0] \quad (3)$$

$$[\omega/\gamma]^2 = H_{\backslash\backslash}[H_{\backslash\backslash} + 4\pi M_0] \quad (4)$$

The demagnetization field and g value of the samples were calculated by solving the above two equations for corresponding values of $H_\perp$ and $H_{\backslash\backslash}$. In the single-layer LSMO films, the calculated g value is 1.97 for all samples. The demagnetization field is 3507 Oe. for 10 nm LSMO film and monotonically increases to 3770 Oe in the case of 40 nm LSMO film. For the bilayer system, a clear distinction can be observed between the primary and the secondary signal. The primary signal has a high value of demagnetization field (3413 Oe. for LY2040) and increases to 3623 Oe. in the LY4040 sample, with the increase in LSMO thickness. But the $4\pi M_0$ is only 49 Oe. in LY2040 for the second signal and remains almost independent of the LSMO layer thickness. Since the small $4\pi M_0$ parameter implies a drastic decrease in magnetization, this result indicates the suppression of magnetization, evident from the magnetization measurement transpired from the weakly magnetic interfacial layer. The g value of the primary signal is close to 2 as expected for a metallic LSMO film, but for the second signal, it is higher than 2.5. The high g value possibly originates from the localized electrons at the interfacial disordered sites.

Figure 4c,d shows the variation of H_{res} for different in-plane orientations (ϕ_H) of the magnetic field measured in bilayer and monolayer samples, respectively. The overlap of two ESR signals is observed for all values of ϕ_H in bilayer samples. However, only one FMR signal is present in the case of single-layer LSMO films, indicating in-plane magnetic homogeneity. The extracted value of H_{res} plotted in Figure 4d shows a strong fourfold anisotropy with the easy axis along the (001) direction in the case of the primary signal in both the bilayer and in the single-layer LSMO sample, reflecting the epitaxial growth.[22] The secondary signal in the bilayer samples exhibits two-fold-like symmetry, indicating a weakly magnetic heterogeneous layer formed at the interface, responsible for the suppression of superconductivity and hybrid pinning mechanism in the bilayer samples.

CONCLUSIONS

In conclusion, we have investigated the effect of LSMO thickness on the magnetic flux pinning properties of YBCO/LSMO bilayer systems. Our study of static magnetization indicates that the suppression of magnetic and superconducting properties in the bilayer samples might be related to the

https://doi.org/10.1021/acsomega.2c07928
ACS Omega 2023, 8, 16694−16699

presence of a weak magnetic layer at the interface between LSMO and YBCO. Analysis of the critical current in the bilayer samples indicates the presence of an additional pinning mechanism besides the normal magnetic pinning by the LSMO layer.

To further probe the magnetic dynamics of these bilayer systems, radiofrequency magnetic resonance spectra were studied. Multiple FMR signals were observed in the bilayer LSMO/YBCO samples. Compared with the epitaxial single-layer LSMO, the second magnetic FMR line in bilayer samples is identified to be emerging from the interfacial magnetic heterogeneity. This investigation prevails a flux pinning mechanism from the interface in addition to magnetic pinning from bulk LSMO, which may create a way for the future applications of ferromagnetic/superconducting hybrid structure.

AUTHOR INFORMATION

Corresponding Author

Jauyn Grace Lin − *Center for Condensed Matter Science, National Taiwan University, Taipei 10617, Taiwan; Center of Atomic Initiatives for New Materials, National Taiwan University, Taipei 10617, Taiwan*; Email: jglin@ntu.edu.tw

Authors

Sayan Chaudhuri − *Center for Condensed Matter Science, National Taiwan University, Taipei 10617, Taiwan;* Present Address: Department of Physics, GITAM School of Science, GITAM (Deemed to be University), Hyderabad, Telangana, 502329, India; orcid.org/0000-0002-2654-3850

You-Sheng Chen − *Center for Condensed Matter Science, National Taiwan University, Taipei 10617, Taiwan*

Complete contact information is available at: https://pubs.acs.org/10.1021/acsomega.2c07928

Notes

The authors declare no competing financial interest.

ACKNOWLEDGMENTS

The authors acknowledge the Ministry of Science and Technology of Taiwan for financial support through Grant Nos. MOST-110-2123-M-002-008 and MOST-110-2112-M-002-041. Part of the funding comes from the National Taiwan University (NTU-110L900803).

REFERENCES

(1) Buzdin, A. I. Proximity Effects in Superconductor-Ferromagnet Heterostructures. *Rev. Mod. Phys.* **2005**, *77*, 935−976.

(2) Bergeret, F. S.; Volkov, A. F.; Efetov, K. B. Odd Triplet Superconductivity and Related Phenomena in Superconductor-Ferromagnet Structures. *Rev. Mod. Phys.* **2005**, *77*, 1321−1373.

(3) Dybko, K.; Werner-Malento, K.; Sawicki, M.; Przyslupski, P. Enhancement of the Superconducting Transition Temperature by an External Magnetic Field Parallel to the Plane of La0.7Sr0.3MnO 3/ YBa2Cu3O7/La0.7Sr 0.3MnO3 Trilayers. *EPL (Europhys. Lett.)* **2009**, *85*, No. 57010.

(4) Przyslupski, P.; Komissarov, I.; Paszkowicz, W.; Dluzewski, P.; Minikayev, R.; Sawicki, M. Structure and Magnetic Characterization of La0.67Sr 0.33MnO3/YBa2Cu3O7 Superlattices. *J. Appl. Phys.* **2004**, *95*, 2906−2911.

(5) Kasai, M.; Kanke, Y.; Ohno, T.; Kozono, Y. Possible Mechanism of Proximity Effect Coupled to Spin Fluctuation in YBa 2 Cu 3 O y /Magnetic Manganese Oxide/YBa 2 Cu 3 O y Junctions. *J. Appl. Phys.* **1992**, *72*, 5344−5349.

(6) Klose, C.; Khaire, T. S.; Wang, Y.; Pratt, W. P.; Birge, N. O.; McMorran, B. J.; Ginley, T. P.; Borchers, J. A.; Kirby, B. J.; Maranville, B. B.; Unguris, J. Optimization of Spin-Triplet Supercurrent in Ferromagnetic Josephson Junctions. *Phys. Rev. Lett.* **2012**, *108*, No. 127002.

(7) Bhatt, H.; Kumar, Y.; Prajapat, C. L.; Kinane, C. J.; Caruana, A.; Langridge, S.; Basu, S.; Singh, S. Correlation of Magnetic and Superconducting Properties with the Strength of the Magnetic Proximity Effect in La 0.67 Sr 0.33 MnO 3 /SrTiO 3 /YBa 2 Cu 3 O 7- Heterostructures. *ACS Appl. Mater. Interfaces* **2022**, *14*, 8565−8574.

(8) Han, F.; Chen, X.; Wang, J.; Huang, X.; Zhang, J.; Song, J.; Liu, B.; Chen, Y.; Bai, X.; Hu, F.; Shen, B.; Sun, J. Perpendicular Magnetic Anisotropy Induced by La2/3Sr1/3MnO3-YBaCo2O5+δinterlayer Coupling. *J. Phys. D: Appl. Phys.* **2021**, *54*, No. 185302.

(9) Zhang, X. X.; Wen, G. H.; Zheng, R. K.; Xiong, G. C.; Lian, G. J. Enhanced Flux Pinning in a High-Tc Superconducting Film by a Ferromagnetic Buffer Layer. *Europhys. Lett. (EPL)* **2001**, *56*, 119−125.

(10) Jha, A. K.; Khare, N.; Pinto, R. Enhanced Critical Current Density in YBa2Cu3O 7-δ Thin Film Deposited on La0.67Sr 0.33MnO3 Decorated SrTiO3 Substrates. *Phys. C* **2011**, *471*, 1154−1157.

(11) Dybko, K.; Werner-Malento, K.; Aleshkevych, P.; Wojcik, M.; Sawicki, M.; Przyslupski, P. Possible Spin-Triplet Superconducting Phase in the La0.7 Sr0.3 MnO3 / YBa2 Cu3 O7 / La0.7 Sr0.3 MnO3 Trilayer. *Phys. Rev. B* **2009**, *80*, No. 144504.

(12) Sefrioui, Z.; Arias, D.; Peña, V.; Villegas, J. E.; Varela, M.; Prieto, P.; León, C.; Martinez, J. L.; Santamaria, J. Ferromagnetic Superconducting Proximity Effect in La0.7Ca0.3MnO3 / YBa2-Cu3O7 Superlattices. *Phys. Rev. B* **2003**, *67*, No. 214511.

(13) Stahn, J.; Chakhalian, J.; Niedermayer, C.; Hoppler, J.; Gutberlet, T.; Voigt, J.; Treubel, F.; Habermeier, H. U.; Cristiani, G.; Keimer, B.; Bernhard, C. Magnetic Proximity Effect in Perovskite Superconductor/Ferromagnet Multilayers. *Phys. Rev. B* **2005**, *71*, No. 140509.

(14) Luo, W.; Pennycook, S. J.; Pantelides, S. T. Magnetic "Dead" Layer at a Complex Oxide Interface. *Phys. Rev. Lett.* **2008**, *101*, No. 247204.

(15) Chakhalian, J.; Freeland, J. W.; Habermeier, H.-U.; Cristiani, G.; Khaliullin, G.; van Veenendaal, M.; Keimer, B. Orbital Reconstruction and Covalent Bonding at an Oxide Interface. *Science* **2007**, *318*, 1114−1117.

(16) Tebano, A.; Orsini, A.; Medaglia, P. G.; Di Castro, D.; Balestrino, G.; Freelon, B.; Bostwick, A.; Chang, Y. J.; Gaines, G.; Rotenberg, E.; Saini, N. L. Preferential Occupation of Interface Bands in La2/3 Sr 1/3 MnO3 Films as Seen via Angle-Resolved Photoemission. *Phys. Rev. B* **2010**, *82*, No. 214407.

(17) de Andrés Prada, R.; Gaina, R.; Biškup, N.; Varela, M.; Stahn, J.; Bernhard, C. Controlling the Strength of Ferromagnetic Order in YB A2 C U3 O7/ L A2/3 C A1/3Mn O3 Multilayers. *Phys. Rev. B* **2019**, *100*, No. 115129.

(18) Wisser, J. J.; Suzuki, Y. Growth and Characterization of La0.67Sr0.33MnO3/YBa2Cu3O7- Δbilayers. *AIP Adv.* **2021**, *11*, No. 015007.

(19) Prajapat, C. L.; Singh, S.; Paul, A.; Bhattacharya, D.; Singh, M. R.; Mattauch, S.; Ravikumar, G.; Basu, S. Superconductivity-Induced Magnetization Depletion in a Ferromagnet through an Insulator in a Ferromagnet-Insulator-Superconductor Hybrid Oxide Heterostructure. *Nanoscale* **2016**, *8*, 10188−10197.

(20) Singh, S.; Bhatt, H.; Kumar, Y.; Prajapat, C. L.; Satpati, B.; Kinane, C. J.; Langridge, S.; Ravikumar, G.; Basu, S. Superconductivity-Driven Negative Interfacial Magnetization in YBa2-Cu3O7-δ/SrTiO3/La0.67Sr0.33MnO3 Heterostructures. *Appl. Phys. Lett.* **2020**, *116*, No. 022406.

(21) Paull, O. H. C.; Pan, Av.; Causer, G. L.; Fedoseev, S. A.; Jones, A.; Liu, X.; Rosenfeld, A.; Klose, F. Field Dependence of the

Ferromagnetic/Superconducting Proximity Effect in a YBCO/STO/LCMO Multilayer. *Nanoscale* **2018**, *10*, 18995−19003.
(22) Mercone, S.; Belmeguenai, M.; Malo, S.; Ott, F.; Cayrel, F.; Golosovsky, M.; Leridon, B.; Adamo, C.; Monod, P. Investigation of Ferromagnetic Heterogeneities in La0.7Sr0.3MnO3 Thin Films. *J. Phys. D: Appl. Phys.* **2017**, *50*, No. 045001.
(23) Gyorgy, E. M.; van Dover, R. B.; Jackson, K. A.; Schneemeyer, L. F.; Waszczak, Jv. Anisotropic Critical Currents in Ba 2 YCu 3 O 7 Analyzed Using an Extended Bean Model. *Appl. Phys. Lett.* **1989**, *55*, 283−285.
(24) Galakhov, V. R.; Demeter, M.; Bartkowski, S.; Neumann, M.; Ovechkina, N. A.; Kurmaev, E. Z.; Lobachevskaya, N. I.; Mukovskii, Y. M.; Mitchell, J.; Ederer, D. L. Mn 3s Exchange Splitting in Mixed-Valence Manganites. *Phys. Rev. B* **2002**, *65*, No. 113102.
(25) Dew-Hughes, D. Flux Pinning Mechanisms in Type II Superconductors. *Philos. Mag.* **1974**, *30*, 293−305.
(26) Oh, J. Y.; Song, C. Y.; Ko, Y. J.; Lee, J. M.; Kang, W. N.; Yang, D. S.; Kang, B. Strong Correlation between Flux Pinning and Epitaxial Strain in the GdBa2Cu3O7-x/La0.7Sr0.3MnO3nanocrystalline Heterostructure. *RSC Adv.* **2020**, *10*, 39102−39108.
(27) Oh, J. Y.; Yang, D. S.; Kang, W. N.; Kang, B. Competition between Ferromagnetism and Superconductivity in GdBa2Cu3O7-x/La0.7Sr0.3MnO3 Bilayers with Varying Thickness. *Ceram. Int.* **2022**, *48*, 1068−1076.
(28) Blatter, G.; Feigel'Man, Mv.; Geshkenbein, V. B.; Larkin, A. I.; Vinokur, V. M. Vortices in High-Temperature Superconductors. *Rev. Mod. Phys.* **1994**, *66*, 1125.
(29) Chen, C. Z.; Liu, Z. Y.; Lu, Y. M.; Zeng, L.; Cai, C. B.; Zeng, R.; Dou, S. X. Robust High-Temperature Magnetic Pinning Induced by Proximity in YBa 2Cu3O7-δ/La0.67Sr 0.33MnO3 Hybrids. *J. Appl. Phys.* **2011**, *109*, No. 073921.

https://doi.org/10.1021/acsomega.2c07928
ACS Omega 2023, 8, 16694−16699